

# Extracting Many-Body Quantum Resources within One-Body Reduced Density Matrix Functional Theory

Carlos L. Benavides-Riveros,<sup>1,\*</sup> Tomasz Wasak,<sup>2,†</sup> and Alessio Recati<sup>1</sup>

<sup>1</sup>*Pitaevskii BEC Center, CNR-INO and Dipartimento di Fisica, Università di Trento, I-38123 Trento, Italy*

<sup>2</sup>*Institute of Physics, Faculty of Physics, Astronomy and Informatics, Nicolaus Copernicus University in Toruń, Grudziądzka 5, 87-100 Toruń, Poland*

(Dated: November 22, 2023)

Quantum Fisher information (QFI) is a central concept in quantum sciences used to quantify the ultimate precision limit of parameter estimation, detect quantum phase transitions, witness genuine multipartite entanglement, or probe nonlocality. Despite this widespread range of applications, computing the QFI value of quantum many-body systems is, in general, a very demanding task. Here we combine ideas from functional theories and quantum information to develop a novel functional framework for the QFI of fermionic and bosonic ground states. By relying upon the constrained-search approach, we demonstrate that the QFI matrix values can universally be determined by the one-body reduced density matrix (1-RDM), avoiding thus the use of exponentially large wave functions. Furthermore, we show that QFI functionals can be determined from the universal 1-RDM functional by calculating its derivatives with respect to the coupling strengths, becoming thus the *generating* functional of the QFI. We showcase our approach with the Bose-Hubbard model and present exact analytical and numerical QFI functionals. Our results provide the first connection between the one-body reduced density matrix functional theory and the quantum Fisher information.

*Introduction.*— The concept of quantum correlations is transversal for many areas of quantum physics ranging from condensed matter [1, 2] and quantum chemistry [3, 4] to high-energy physics [5, 6]. Among different measures of quantum correlations, the quantum Fisher information (QFI) [7] is a key quantity that not only gives an operational meaning for multipartite entanglement for quantum-enhanced metrology of spins [8], bosons [9, 10] and fermions [11], but can also be used to probe quantum criticality [12, 13], nonlocality [14–16], and quantum geometry [17]. This widespread range of applications makes QFI a fundamentally important concept in quantum physics [18–21]. However, due to the problem of finding an optimal measurement which yields the QFI, its determination in quantum many-body systems remains an important theoretical and technological challenge [22, 23].

Experimentally, the value of the QFI was extracted, in the form of a lower bound, and used to prove entanglement of non-Gaussian many-body states [24] and pair-correlated states of twin matter waves [25]. For thermal states, the QFI was directly related to dynamic susceptibilities [13] and to the quench dynamics in linear response [11]. With the former method, the QFI was measured and used to quantify entanglement in a spin-1/2 Heisenberg antiferromagnetic chain [26] and for nitrogen-vacancy center in diamonds [27]. Recently, a method to determine the optimal use of a given entangled state for quantum sensing was proposed based on the QFI matrix (QFIM) [28] showing its usefulness to determine optimal quantum technology protocols. Despite this experimental progress, extracting quantum correlations in many-body systems, and, thus, quantifying their quantum re-

sources through QFI, is still hampered by the Hilbert space’s exponential growth, rendering the computation a formidably demanding task [29, 30].

A strategy to alleviate the cost of computing global quantities of quantum many-body systems is to estimate them from local measurements. For instance, artificial neural networks can be trained to learn the entanglement entropy or the two-point density correlations of interacting fermions from local correlations [31–35]. The intuition behind this is that some physical properties of quantum systems (usually the ones of ground states) can unambiguously be determined by certain reduced quantities. Many rigorous theorems establish the existence of one-to-one maps between ground states  $|\psi\rangle$  and appropriately chosen sets of reduced quantities  $\{\omega_\mu\}$ , such as the particle density or the reduced density matrix, justifying thus the *functional* notation  $|\psi[\{\omega_\mu\}]\rangle$  [36–40]. As a consequence, all observables of the system’s ground state are also implicitly functionals of those reduced quantities. Yet, while this is true, almost all research in functional theories focuses on developing energy functionals [41–51]. Questions about multipartite quantum correlations or nonlocality in the systems these functionals describe are usually neither addressed nor even posed [52].

Here we initiate and develop a functional-theoretical framework for the QFI. We will show that for ground states of identical particles the QFIM can be determined by the one-body reduced density matrix (1-RDM)  $\gamma$ , obtained by tracing out  $N - 1$  particles of the  $N$ -body quantum state, avoiding thus the pre-computation of wave functions that expand into exponentially large Hilbert spaces. We will unveil two surprising links between the one-body reduced density matrix functional theory (1-RDMFT) and the QFI functional theory introduced in this work: (i) *QFI functionals correspond to the derivatives of the 1-RDM functionals with respect to the cou-*

\* cl.benavidesriveros@unitn.it

† twasak@umk.pl

pling strengths, revealing the ability of 1-RDMFT to capture itself quantum correlations, and (ii) *the energy functional of the 1-RDM can be fully reconstructed from the functionals of the QFI*.

The paper is structured as follows: First, we present a general framework for the functional theory of the 1-RDM and recap the concept of QFIM. Next, we present the main ingredients of our novel functional theory of QFI, showcasing our approach for a Bose-Hubbard model. We finish with conclusions. Three additional appendices contain additional technical details.

*Hubbard-like Hamiltonian.* — We begin with the Hamiltonian:

$$\hat{H} = \hat{h} + \hat{W}. \quad (1)$$

The one-body part  $\hat{h} = -\sum_{\langle ij \rangle} t_{ij} \hat{b}_i^\dagger \hat{b}_j$  describes the tunneling, while the two-body term is of the general form

$$\hat{W} = \frac{1}{2} \sum_{ijkl} V_{ijkl} \hat{b}_i^\dagger \hat{b}_j^\dagger \hat{b}_k \hat{b}_l. \quad (2)$$

The operators  $\hat{b}_j^\dagger$  ( $\hat{b}_j$ ) create (annihilate) a particle on site  $j$ . For a standard Hubbard model with on-site interaction, the couplings are nonzero only when all the indices are equal  $V_{jjjj} = U$ . We keep the general matrix elements to take into account non-standard Hubbard models accounting, for example, for dipolar couplings [53]. For notational convenience and in order to relate the functional formalism to quantum information concepts, we define site-dependent angular-momentum Hermitian operators, i.e.,  $\hat{J}_\alpha^{ij} = \frac{1}{2}(\hat{b}_i^\dagger, \hat{b}_j^\dagger) \sigma_\alpha (\hat{b}_i, \hat{b}_j)^T$ , where  $\sigma_\alpha$ , with  $\alpha = 0, x, y, z$ , are Pauli matrices. The two-body operator (2) can be rewritten, up to a one-body operator that can be incorporated into  $h$ , as

$$\hat{W} = \sum_{\alpha, \beta} \sum_{ijkl} u_{\alpha\beta}^{ijkl} \{\hat{J}_\alpha^{ij}, \hat{J}_\beta^{kl}\}, \quad (3)$$

where  $\{A, B\} = AB + BA$  and  $u_{\alpha\beta}^{ijkl}$  are real coupling strengths subject to additional constraints stemming from the symmetry of the operators  $\{\hat{J}_\alpha^{ij}, \hat{J}_\beta^{kl}\}$ .

Our central result is that (3) leads to a universal functional  $\mathcal{F}[\gamma; \mathbf{u}]$ , with  $\mathbf{u} = \{u_{\alpha\beta}^{ij}\}$ , that serves as a generating functional of the QFI. We first introduce both concepts ( $\mathcal{F}$  and QFI) and then show this connection.

*One-body reduced-density-matrix functional theory.* — Given a  $N$ -body density matrix  $\rho$ , we define the 1-RDM as

$$\gamma_\alpha^{ij} \equiv \text{Tr}[\rho \hat{J}_\alpha^{ij}]. \quad (4)$$

Here,  $(\alpha, i, j)$  is the collective index of the vector  $\gamma$ . Although this representation of  $\gamma$  is not standard [54], it will be convenient to develop our functional formulation of QFI. The ground-state problem for a many-body Hamiltonian of the form in Eq. (1) can be solved without resorting to wave functions by proving the existence of

a 1-RDM-functional  $\mathcal{F}[\gamma]$  [39], which describes the two-body interactions in terms of  $\gamma$ : for any choice of  $h$  the ground-state 1-RDM follows from the minimization of  $\mathcal{E}[\gamma] = \text{Tr}[h\gamma] + \mathcal{F}[\gamma]$ , where the first term depends linearly on  $\gamma$ . Since the functional  $\mathcal{F}[\gamma]$  depends only on the *fixed* interaction  $W$  (not on the one-particle Hamiltonians) it is called *universal* [55]. The *constrained-search approach* [56] indicates a route for the calculation of  $\mathcal{F}[\gamma]$  by minimizing the expectation value of the interacting energy over all states  $|\psi\rangle$  that lead to the same  $\gamma$ . Symbolically,

$$\mathcal{F}[\gamma] = \min_{\psi \rightarrow \gamma} \langle \psi | \hat{W} | \psi \rangle. \quad (5)$$

Explicit calculations of this functional have been carried out for bosons [57–60] and fermions [49, 61, 62]. The minimizers  $|\psi[\gamma]\rangle = \text{argmin}_{\psi \rightarrow \gamma} \langle \psi | \hat{W} | \psi \rangle$  do not only correspond to ground states but to the entire set of (representable) 1-RDMs [63].

Crucially, for  $W$  from Eq. (3), the functional not only depends on the 1-RDM but also on the set of coupling constants. This fact seems to be missed in the literature, and below we show how the QFI can be extracted from  $\mathcal{F}$  when the latter is considered as a generating functional. To this end, we introduce the following general notation:

$$\mathcal{F}[\gamma; \mathbf{u}] \equiv \min_{\psi \rightarrow \gamma} \sum_{\alpha, \beta} \sum_{ijkl} u_{\alpha\beta}^{ijkl} \langle \psi | \{\hat{J}_\alpha^{ij}, \hat{J}_\beta^{kl}\} | \psi \rangle. \quad (6)$$

*Quantum Fisher information.* — Consider a transformation of the density matrix  $\rho$ , describing the state of the quantum system, using a unitary operator  $\hat{U}(\phi)$ . The resulting state becomes  $\rho(\phi) = \hat{U}(\phi)\rho\hat{U}^\dagger(\phi)$ . The distance between these two density matrices (and the response of the quantum state to perturbations) can be quantified by the QFI. Specifically, for the response  $\partial\rho(\phi)/\partial\phi_a \equiv (\rho\hat{L}_a + \hat{L}_a\rho)/2$ , where  $\hat{L}_a$  is called the Symmetric Logarithmic Derivative and  $\phi_a$  is the  $a$ -th parameter of the vector  $\phi$ , the QFIM is  $M_{ab} = \text{Tr}[\rho\hat{L}_a\hat{L}_b]$ . Since large QFI implies high sensitivity, originally the QFI was introduced in the context of quantum metrology and sensing via the quantum Cramér-Rao lower bound, which quantifies the ultimate precision limit in estimation protocols [64–66].

We parametrize the unitary with the angular-momentum operators, i.e.,  $\hat{U}(\phi) = \exp(i\sum_\alpha \sum_{ij} \phi_\alpha^{ij} \hat{J}_\alpha^{ij})$ . For pure states, which are considered in this work,  $\rho = |\psi\rangle\langle\psi|$ , the QFIM becomes the covariance matrix

$$M_{\alpha\beta}^{ijkl}[\psi] = 2\langle\psi|\{\hat{J}_\alpha^{ij}, \hat{J}_\beta^{kl}\}|\psi\rangle - 4\langle\psi|\hat{J}_\alpha^{ij}|\psi\rangle\langle\psi|\hat{J}_\beta^{kl}|\psi\rangle. \quad (7)$$

An impediment to the calculation of this matrix is the prior knowledge of the quantum state, which involves computations of such complexity that hampers broad applicability. This problem, we will now see, can be circumvented by relying upon the 1-RDMs and the universal functional  $\mathcal{F}$ .

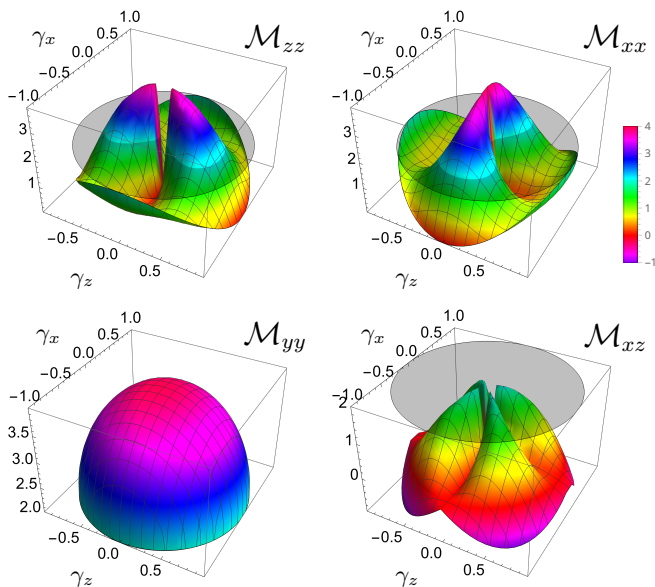


FIG. 1: Universal functionals of QFIM for the repulsive Bose-Hubbard model (for all  $U > 0$ ) for  $N = 2$ . The limit  $\mathcal{M}_{\alpha\beta} = 2$  is indicated as a disk in gray.

We note that the QFI is an entanglement measure [9, 10]: for a quantum system of  $N$  bosons or spins, the state exhibits at least  $(m + 1)$ -particle entanglement [67] if the single-parameter QFI surpasses the quantum limit, e.g.,  $\sum_{\alpha\beta} n_{\alpha} n_{\beta} M_{\alpha\beta}^{ijij} > sm^2 + (N - sm)^2$ , where  $s$  is an integer part of  $N/m$ , and  $m = 1, 2, 3, \dots$  quantifies entanglement depth; the vector  $n$  is normalized,  $\sum_{\alpha} n_{\alpha}^2 = 1$ . For  $m = 1$ , the right-hand side, equal to  $N$ , is the standard quantum limit [22]. Similar inequality was derived for fermions [11]. If the inequality is violated, the entanglement structure is not revealed.

*Functional theory of QFIM.*— The central quantity of the framework presented above is the 1-RDM. Noteworthy, it already contains information about quantum correlations, via the correlation entropy  $S[\gamma] = -\text{Tr}[\gamma \ln \gamma]$  [31, 68–70]. Surprisingly, 1-RDMFT is mainly focused on the goal of computing the ground-state energy and some associated observables [54, 71–76], but this powerful formalism has not been used to scrutiny multipartite entanglement or nonlocality. Indeed, the map  $\gamma \rightarrow |\psi[\gamma]\rangle$  can be used for the calculation of functionals of QFIM: by using Eq. (7) one can view QFIM as explicitly, universal functionals dependent on the 1-RDM:

$$\mathcal{M}_{\alpha\beta}^{ijkl}[\gamma] \equiv M_{\alpha\beta}^{ijkl}[\psi[\gamma]]. \quad (8)$$

Let's emphasize that this functional is defined in a domain whose degrees of freedom do not scale with the number of particles. We now explain how  $M_{\alpha\beta}^{ijkl}$  can be directly obtained from the universal functional  $\mathcal{F}$ .

*Generation of QFI and reconstruction of  $\mathcal{F}$ .*— The universal functional is a function of the couplings  $\mathbf{u}$ , cf. Eq. (6). By applying the Hellmann-Feynman theorem to

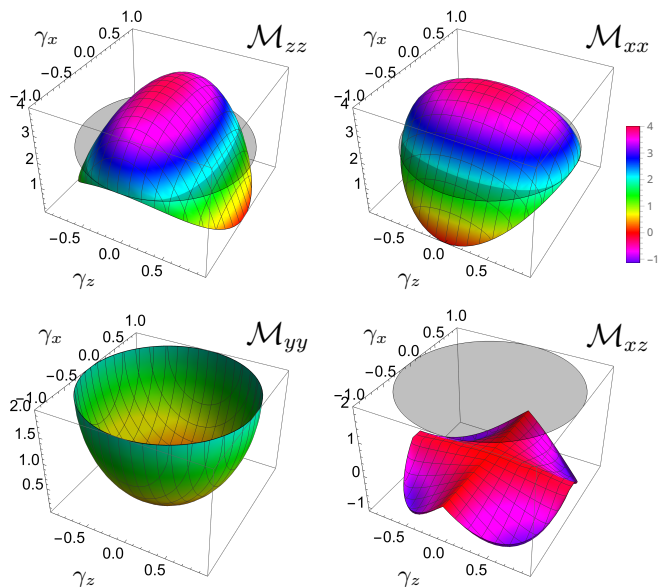


FIG. 2: Universal functionals of QFIM for the attractive Bose-Hubbard model (for all  $U < 0$ ) for  $N = 2$ . The limit  $\mathcal{M}_{\alpha\beta} = 2$  is indicated as a disk in gray.

the derivative of the functional [77], we show, as detailed in Appendix C, that  $\mathcal{M}$  can be generated by the total energy functional  $\mathcal{E}$  by means of the relation

$$\mathcal{M}_{\alpha\beta}^{ijkl}[\gamma; \mathbf{u}] = 4 \left[ \left( \frac{\partial \mathcal{E}[\gamma; \mathbf{u}]}{\partial u_{\alpha\beta}^{ijkl}} \right)_{\gamma} - \gamma_{\alpha}^{ij} \gamma_{\beta}^{kl} \right], \quad (9)$$

where  $\gamma$  is kept fixed in the derivative and we indicated that  $\mathcal{M}$  depends on  $\mathbf{u}$ . We note that one can substitute here  $\mathcal{F}$  instead of  $\mathcal{E}$ , but the latter is accessible experimentally. This is our central result, which shows that, once the universal functional is determined as a function of the coupling strengths, it provides access to quantum resources quantified by the QFI without referring to the quantum state  $|\psi[\gamma]\rangle$ .

Furthermore, the average of Eq. (3) with respect to  $|\psi[\gamma]\rangle$  yields the relation

$$\mathcal{F}[\gamma; \mathbf{u}] = \sum_{\alpha\beta} \sum_{ijkl} u_{\alpha\beta}^{ijkl} \left( \frac{1}{4} \mathcal{M}_{\alpha\beta}^{ijkl}[\gamma; \mathbf{u}] + \gamma_{\alpha}^{ij} \gamma_{\beta}^{kl} \right). \quad (10)$$

Hence, the QFIM, together with its content about quantum resources, enters into the universal functional. These results show that the knowledge of the QFIM allows for full reconstruction of the universal 1-RDM functional.

*Two-well Bose-Hubbard model.*— Two-well Hubbard models played a historical role as analytical tests for density functional theory in its ground-state [78], time-dependent [79], and excited-state ensemble [80] versions in order to unveil analytical properties of the functionals [57, 62, 81, 82]. It was already used in the context of bosonic Josephson Junctions to obtain quantum resources in terms of spin squeezing and QFI [24, 83]. An

advantage of the bosonic model is that, while it can be filled with an arbitrary number of particles, the functionals can be visualized as 3D graphs. The Hamiltonian is:

$$\hat{H} = -t \sum_{\langle ij \rangle} \hat{b}_i^\dagger \hat{b}_j + u \sum_j \hat{n}_j (\hat{n}_j - 1), \quad (11)$$

where  $\hat{n}_j = \hat{b}_j^\dagger \hat{b}_j$  is the particle-number operator in the site  $j = r$  (right) or  $l$  (left); the on-site interactions in Eq. (2) are  $V_{rrrr} = V_{llll} = u$  and the rest are zero. The term  $\hat{W} = u \sum_{j \in \{l,r\}} \hat{n}_j (\hat{n}_j - 1)$  is the relevant quantity of what follows. As only two sites are considered we drop the site indices:

$$\gamma_\alpha = \langle \psi | \hat{J}_\alpha | \psi \rangle, \quad (12)$$

with  $\sum_\alpha \gamma_\alpha^2 \leq N^2/4$ . This means that all 1-RDMs lie inside the Bloch sphere of radius  $N/2$ .

The universal functional contains all the information to reconstruct one of the diagonals of the QFIM. This is a consequence of the relation between  $\hat{W}$  and  $\hat{J}_z$ :

$$\sum_{j \in \{l,r\}} \hat{n}_j (\hat{n}_j - 1) = 2\hat{J}_z^2 + \frac{\hat{N}^2}{2} - \hat{N}, \quad (13)$$

where  $\hat{N} = \hat{n}_l + \hat{n}_r$ . Hence, since  $|\psi\rangle$  has a fixed number of particles, we obtain:  $\langle \psi | \hat{W} | \psi \rangle / u = 2\langle \psi | \hat{J}_z^2 | \psi \rangle + N^2/2 - N$ . By replacing  $\psi \rightarrow \psi[\gamma]$ , it follows

$$\mathcal{M}_{zz}[\gamma] = 4 \left( \frac{\mathcal{F}[\gamma; u]}{u} - \gamma_z^2 \right) - N^2 + 2N, \quad (14)$$

which is a special case of Eq. (9) with a single coupling strength. It is instructive to write the expression of the functional for  $N = 2$ . With real wave functions ( $\gamma_y = 0$ ),

$$\mathcal{M}_{zz}[\gamma] = 4 \left[ 1 - \frac{1 + \sqrt{1 - (\gamma_x^2 + \gamma_z^2)}}{2(\gamma_x^2 + \gamma_z^2)} \gamma_x^2 - \gamma_z^2 \right]. \quad (15)$$

In Fig. 1 the exact functionals for  $\mathcal{M}_{xx}$ ,  $\mathcal{M}_{yy}$ ,  $\mathcal{M}_{zz}$  and  $\mathcal{M}_{xz}$  are presented for  $U > 0$ . Since the amplitudes of the wavefunctions are real and  $\{\hat{J}_x, \hat{J}_y\}$  and  $\{\hat{J}_y, \hat{J}_z\}$  are skew symmetrical operators,  $\mathcal{M}_{xy} = \mathcal{M}_{yz} = 0$ , everywhere. With a gray disk, we mark the value of the standard quantum limit and thus the values  $\mathcal{M}_{\alpha\alpha} > N = 2$  signal entanglement. We observe that for  $\mathcal{M}_{yy}$ , all the states are entangled apart from the surface of the Bloch sphere, describing spin coherent states, at which the quantum limit is not surpassed also for  $\alpha = x, z$ , i.e.,  $\mathcal{M}_{\alpha\alpha} \leq N$ .

We notice that the above results are valid for repulsive interaction, and, therefore, not all quantum states can become a minimizer. For instance, the NOON state  $(|2, 0\rangle + |0, 2\rangle)/\sqrt{2}$  shows up in the functionals with attractive interactions  $U < 0$ . They are sketched in Fig. 2. While some features are similar, they differ greatly from the functionals in Fig. 1: for the attractive case, the value of the QFI of most of the ground states lies above the

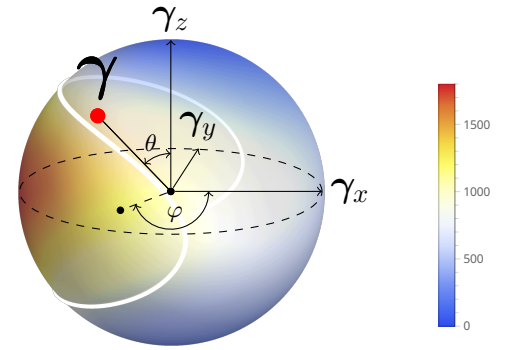


FIG. 3: Representation of  $\gamma$ , parametrized with the angles  $\theta$  and  $\varphi$ , inside the Bloch sphere of radius  $N/2$ . The color-code represents the value of  $\mathcal{M}_{zz}$  close to BEC for  $N = 1000$  and  $\delta = 0.1$  (see Eq. (16)). The white line marks the standard quantum limit  $\mathcal{M}_{zz} = N$ .

quantum limit, although there are states *within* the Bloch sphere which do not exhibit entanglement.

*QFIM functional theory for BEC.*— Another interesting limit of the two-well Bose-Hubbard model is the Bose-Einstein condensate (BEC) state, which has been used for quantum metrological tasks, spin squeezing and test Bell correlations [84–87]. Due to the Penrose-Onsager criterion [88], BEC states lie near the border of the Bloch sphere and it is convenient to define the functionals in terms of the angles  $\theta$  and  $\varphi$ , and the number of particles depleted from the condensate (i.e., away from the set of spin coherent states):  $\delta = N/2 - \gamma$  (see Fig. 3). Thus, the QFIM functionals can be expressed as functions of the spherical coordinates  $\mathcal{M}_{\alpha\beta}(\delta, \theta, \varphi)$ . In the neighborhood of the condensation point,  $\mathcal{M}_{zz}$  reads (see Appendix B):

$$\mathcal{M}_{zz}(\delta, \theta, \varphi) = \mathcal{M}_{zz}^{(0)}(\theta) - \mathcal{M}_{zz}^{(1/2)}(\theta, \varphi)\delta^{1/2} + \mathcal{M}_{zz}^{(1)}(\theta)\delta + \mathcal{O}(\delta^{3/2}). \quad (16)$$

Here,  $\mathcal{M}_{zz}^{(0)}(\theta) = N \sin^2(\theta)$  represents the mean-field fluctuations which cannot surpass the standard quantum limit, i.e.,  $\mathcal{M}_{zz}^{(0)}(\theta) \leq N$ , whereas the two beyond-mean field corrections scaling as  $\delta^{1/2}$  and  $\delta$  are  $\mathcal{M}_{zz}^{(1/2)}(\varphi, \theta) = 2 \sin^2(\theta) \cos(\varphi) \sqrt{N(N-1)}$  and  $\mathcal{M}_{zz}^{(1)}(\theta) = 8 + 2(N-6) \sin^2(\theta)$ , respectively. The square-root scaling of the second term in Eq. (16) yields the diverging BEC force, that drives nonperturbatively the system away from the mean-field state [57–59]. Since the first term does not violate the standard quantum limit, only the next orders can contribute to genuine multipartite entanglement. In Fig. 3 an example of  $\mathcal{M}_{zz}(\delta, \theta, \varphi)$  is shown for  $N = 1000$  and for depletion  $\delta = 0.1$ . To surpass the standard quantum limit, the mean field contribution should be large, and thus  $\theta \approx \pi/2$ , so  $\gamma$  lies close to the equator. Next, the third term in Eq. (16) is always positive, but is significantly overshadowed by the second term in the region  $\cos \varphi > 0$ . However, in the region  $\cos \varphi < 0$  it contributes

positively, and we observe enhancement of entanglement.

*Conclusion.*— In this paper we combined ideas from functional theories and quantum information to develop a functional approach to the QFI. In our formalism the elements of the QFI matrix are *functionals* of the 1-RDM, avoiding thus the exponential growth of the Hilbert space in which they are usually defined. We obtained two main results: (i) *the knowledge of the QFIM allows the full reconstruction of the universal functional of the 1-RDM* and (ii) *QFI functionals correspond to the derivatives of the 1-RDM functional with respect to the coupling strengths*, the latter being upgraded to the level of generating functional of the QFI functionals. These results show a so far unexplored ability of the 1-RDM functionals to detect genuine multipartite entanglement. Since in 1-RDM functional theory approach, we can freely adjust single-particle Hamiltonians to move in the landscape of the functionals, our work shows a novel way to extract many-body resources and to determine optimal sensing protocols [28].

We leave for future work to exploit our results in the context of quantum chemistry or condensed matter to investigate the use of strongly interacting systems for quantum metrological tasks.

## ACKNOWLEDGMENTS

We acknowledge the European Union's Horizon Europe Research and Innovation program under the Marie Skłodowska-Curie grant agreement n°101065295 (C.L.B.-R.). This research is part of the project No. 2021/43/P/ST2/02911 co-funded by the National Science Centre and the European Union's Horizon 2020 research and innovation programme under the Marie Skłodowska-Curie grant agreement no. 945339. For the purpose of Open Access, the author has applied a CC-BY public copyright licence to any Author Accepted Manuscript (AAM) version arising from this submission.

## Appendix A: Functional theory of quantum Fisher information for the two-site Bose-Hubbard model

We consider a system of  $N$  bosonic particles interacting by the following Hamiltonian:

$$\hat{W} = u \sum_{j=l,r} \hat{n}_j (\hat{n}_j - 1). \quad (\text{A1})$$

We write the 1-RDMs in terms of the following components:  $\gamma_\alpha = \langle \psi | \hat{J}_\alpha | \psi \rangle$ , for  $\alpha = x, y, z$ . In terms of the Pauli matrices  $\sigma_\alpha$ ,

$$\hat{J}_\alpha = \frac{1}{2} \hat{\Psi}^\dagger \sigma_\alpha \hat{\Psi}, \quad (\text{A2})$$

with  $\hat{\Psi}^\dagger \equiv (\hat{b}_l^\dagger, \hat{b}_r^\dagger)$ . A basis of the Hilbert space for  $N$  particles is the following:

$$|n, N-n\rangle = \frac{1}{\sqrt{n!(N-n)!}} (b_l^\dagger)^n (b_r^\dagger)^{N-n} |0\rangle. \quad (\text{A3})$$

By denoting the real-valued expansion coefficients by  $\alpha_n$  and fixing the number of particles to 2, the 1-RDM reads  $\gamma_x = \sqrt{2}\alpha_1(\alpha_0 + \alpha_2)$ ,  $\gamma_y = 0$ , and  $\gamma_z = (\alpha_0^2 - \alpha_2^2)$ . It follows that  $\sqrt{2}\gamma_z\alpha_1/\gamma_x = (\alpha_0 - \alpha_2)$  and  $\gamma_x/\sqrt{2}\alpha_1 = \alpha_0 + \alpha_2$ . One can now write the amplitudes in terms of the 1-RDM. To show this, note first that

$$\alpha_1^2 = \frac{1 \pm \sqrt{1 - (\gamma_x^2 + \gamma_z^2)}}{2(\gamma_x^2 + \gamma_z^2)} \gamma_x^2. \quad (\text{A4})$$

Due to the rotational symmetry of the result, we define  $\gamma_\rho^2 = \gamma_x^2 + \gamma_z^2$ , and  $\gamma_x = \gamma_\rho \sin(\theta)$ . One gets the expression:

$$\alpha_1^2 = \frac{1}{2} \left( 1 \pm \sqrt{1 - \gamma_\rho^2} \right) \sin^2(\theta). \quad (\text{A5})$$

Since  $u$  factories in the two-body interaction, the only important quantity is the sign of the interaction. As a result,

$$\mathcal{F}(\gamma) = \min_{\psi \rightarrow \gamma} \langle \psi | \hat{W} | \psi \rangle = \min \left\{ 2u \left[ 1 - \frac{1}{2} \left( 1 \pm \sqrt{1 - \gamma_\rho^2} \right) \sin^2(\theta) \right] \right\} = u \left[ 2 - \left( 1 + \text{sign}(u) \sqrt{1 - \gamma_\rho^2} \right) \sin^2(\theta) \right]. \quad (\text{A6})$$

By defining

$$\beta_u^2(\gamma_x, \gamma_z) = \frac{1}{2} \frac{1 + \text{sign}(u) \sqrt{1 - (\gamma_x^2 + \gamma_z^2)}}{\gamma_x^2 + \gamma_z^2} \gamma_x^2, \quad (\text{A7})$$

one can write all amplitudes in terms of  $\gamma$  as follows:

$$\alpha_0(\gamma_x, \gamma_z) = \frac{1}{2} \left( \frac{\gamma_x}{\sqrt{2}\beta_u} + \frac{\sqrt{2}\gamma_z\beta_u}{\gamma_x} \right), \quad (\text{A8})$$

$$\alpha_2(\gamma_x, \gamma_z) = \frac{1}{2} \left( \frac{\gamma_x}{\sqrt{2}\beta_u} - \frac{\sqrt{2}\gamma_z\beta_u}{\gamma_x} \right). \quad (\text{A9})$$

With these results at hand, we can now compute the QFIM. First, let's write explicitly the wave function:

$$|\psi(\gamma_x, \gamma_z)\rangle = \alpha_0(\gamma_x, \gamma_z)|2, 0\rangle + \beta_u(\gamma_x, \gamma_z)|1, 1\rangle + \alpha_2(\gamma_x, \gamma_z)|0, 2\rangle, \quad (\text{A10})$$

with  $\alpha_0(\gamma_x, \gamma_z)$ ,  $\beta_u(\gamma_x, \gamma_z)$ , and  $\alpha_2(\gamma_x, \gamma_z)$  as defined in Eqs. A7, A8, and A9, respectively. Recall the angular momentum matrices for this problem:

$$J_x = \frac{1}{\sqrt{2}} \begin{pmatrix} 0 & 1 & 0 \\ 1 & 0 & 1 \\ 0 & 1 & 0 \end{pmatrix}, \quad J_y = \frac{1}{\sqrt{2}i} \begin{pmatrix} 0 & 1 & 0 \\ -1 & 0 & 1 \\ 0 & -1 & 0 \end{pmatrix} \quad \text{and} \quad J_z = \begin{pmatrix} 1 & 0 & 0 \\ 0 & 0 & 0 \\ 0 & 0 & -1 \end{pmatrix}. \quad (\text{A11})$$

Thus, all elements of QFIM can eventually be computed:

$$\begin{aligned} \mathcal{M}_{zz}(\gamma_x, \gamma_z) &= 4\langle\psi(\gamma_x, \gamma_z)|\hat{J}_z^2|\psi(\gamma_x, \gamma_z)\rangle - 4\gamma_z^2 = 4[1 - \beta_u^2(\gamma_x, \gamma_z)] - 4\gamma_x^2, \\ \mathcal{M}_{yy}(\gamma_x, \gamma_z) &= 4\langle\psi(\gamma_x, \gamma_z)|\hat{J}_y^2|\psi(\gamma_x, \gamma_z)\rangle - 4\gamma_y^2 = 2[1 + \beta_u^2(\gamma_x, \gamma_z)] - 4\alpha_0(\gamma_x, \gamma_z)\alpha_2(\gamma_x, \gamma_z), \\ \mathcal{M}_{xx}(\gamma_x, \gamma_z) &= 4\langle\psi(\gamma_x, \gamma_z)|\hat{J}_x^2|\psi(\gamma_x, \gamma_z)\rangle - 4\gamma_x^2 = 2[1 + \beta_u^2(\gamma_x, \gamma_z)] + 4\alpha_0(\gamma_x, \gamma_z)\alpha_2(\gamma_x, \gamma_z) - 4\gamma_x^2, \\ \mathcal{M}_{xz}(\gamma_x, \gamma_z) &= 2\langle\psi(\gamma_x, \gamma_z)|\hat{J}_z\hat{J}_x + \hat{J}_x\hat{J}_z|\psi(\gamma_x, \gamma_z)\rangle - 4\gamma_x\gamma_z = 2\sqrt{2}\beta_u(\gamma_x, \gamma_z)[\alpha_0(\gamma_x, \gamma_z) - \alpha_2(\gamma_x, \gamma_z)] - 4\gamma_x\gamma_z, \end{aligned}$$

and  $\mathcal{M}_{xy}(\gamma_x, \gamma_z) = \mathcal{M}_{yz}(\gamma_x, \gamma_z) = 0$ .

## Appendix B: Functional theory of quantum Fisher information for Bose-Einstein condensates

In this section, we first recap the known results for the two-site Bose-Hubbard model of Refs. [57, 59] and then extend them to compute the QFIM. The interacting Hamiltonian of the system is given in Eq. (A1). We denote the 1-RDM by  $\gamma$  and trace-normalize to the number of particles  $N$ . As  $\gamma = (\gamma_x, \gamma_y, \gamma_z)$  lies in the interior of a sphere of radius  $N/2$ , it can be expressed as a function of the spherical coordinates  $(\rho, \theta, \alpha)$ ,  $\gamma \equiv \gamma(\rho, \theta, \alpha)$ . To be more specific, the cartesian components of the 1-RDM take the form:

$$\begin{aligned} \gamma_z(\gamma_\rho, \theta, \varphi) &= \gamma_\rho \cos(\theta), \\ \gamma_x(\gamma_\rho, \theta, \varphi) &= \gamma_\rho \sin(\theta) \cos(\varphi), \\ \gamma_y(\gamma_\rho, \theta, \varphi) &= \gamma_\rho \sin(\theta) \sin(\varphi). \end{aligned} \quad (\text{B1})$$

Let us perform the following rotation of the original creation/annihilation operators (on the basis of sites):

$$\begin{aligned} \hat{a}_\rho^\dagger &= \cos(\theta/2)\hat{b}_l^\dagger + e^{-i\varphi}\sin(\theta/2)\hat{b}_r^\dagger, \\ \hat{a}_\theta^\dagger &= -e^{i\varphi}\sin(\theta/2)\hat{b}_l^\dagger + \cos(\theta/2)\hat{b}_r^\dagger. \end{aligned} \quad (\text{B2})$$

In this new basis, states of the form

$$|N - n, n\rangle_\rho \equiv \frac{1}{\sqrt{(N-n)!n!}} (a_\rho^\dagger)^{N-n} (a_\theta^\dagger)^n |0\rangle, .$$

map to 1-RDMs with the same  $\varphi$  and  $\theta$ , i.e.,  $\gamma((N-2n)/2, \theta, \varphi)$ . To see this notice that  $\text{Tr}_{N-1}[|N-n, n\rangle\langle N-n, n|] = (N-n)|\rho\rangle\langle\rho| + n|\theta\rangle\langle\theta|$ . Using  $2\cos(\theta/2)\sin(\theta/2) = \sin\theta$  and  $\cos^2(\theta/2) - \sin^2(\theta/2) = \cos(\theta)$ , one easily confirm that

$$\begin{aligned} \gamma_z &= \frac{1}{2}\langle N-n, n|b_l^\dagger b_l - b_r^\dagger b_r|N-n, n\rangle \\ &= \frac{1}{2}(N-n)\langle 0|a_\rho(b_l^\dagger b_l - b_r^\dagger b_r)a_\rho^\dagger|0\rangle + \frac{1}{2}n\langle 0|a_\theta(b_l^\dagger b_l - b_r^\dagger b_r)a_\theta^\dagger|0\rangle = \frac{N-2n}{2}\cos(\theta). \end{aligned} \quad (\text{B3})$$

In the same way, one can see that  $\gamma_x = \frac{N-2n}{2} \sin(\theta) \cos(\varphi)$  and  $\gamma_y = \frac{N-2n}{2} \sin(\theta) \sin(\varphi)$ , which proves our statement.

By noticing that  $\hat{n}_l = \cos^2(\theta/2)\hat{n}_\theta + \sin^2(\theta/2)\hat{n}_\rho - \cos(\theta/2)\sin(\theta/2)(e^{i\varphi}\hat{a}_\rho^\dagger\hat{a}_\theta + e^{-i\varphi}\hat{a}_\theta^\dagger\hat{a}_\rho)$  and  $\hat{n}_r = \sin^2(\theta/2)\hat{n}_\theta + \cos^2(\theta/2)\hat{n}_\rho + \cos(\theta/2)\sin(\theta/2)(e^{i\varphi}\hat{a}_\rho^\dagger\hat{a}_\theta + e^{-i\varphi}\hat{a}_\theta^\dagger\hat{a}_\rho)$ , one gets for the Hamiltonian (A1) in the new basis:

$$\begin{aligned}
\hat{n}_r^2 + \hat{n}_l^2 &= (\cos^4(\theta/2) + \sin^4(\theta/2))(\hat{n}_\theta^2 + \hat{n}_\rho^2) + 2\cos^2(\theta/2)\sin^2(\theta/2)(e^{i\varphi}\hat{a}_\rho^\dagger\hat{a}_\theta + e^{-i\varphi}\hat{a}_\theta^\dagger\hat{a}_\rho)^2 + 4\cos^2(\theta/2)\sin^2(\theta/2)\hat{n}_\rho\hat{n}_\theta \\
&\quad - (\cos^2(\theta/2) - \sin^2(\theta/2))\cos(\theta/2)\sin(\theta/2)\left[(e^{i\varphi}\hat{a}_\rho^\dagger\hat{a}_\theta + e^{-i\varphi}\hat{a}_\theta^\dagger\hat{a}_\rho)\hat{n}_\theta + h.c.\right] \\
&\quad + (\cos^2(\theta/2) - \sin^2(\theta/2))\cos(\theta/2)\sin(\theta/2)\left[(e^{i\varphi}\hat{a}_\rho^\dagger\hat{a}_\theta + e^{-i\varphi}\hat{a}_\theta^\dagger\hat{a}_\rho)\hat{n}_\rho + h.c.\right] \\
&= (1 - \frac{1}{2}\sin^2(\theta))(\hat{n}_\theta^2 + \hat{n}_\rho^2) + \frac{1}{2}\sin^2(\theta)(e^{i\varphi}\hat{a}_\rho^\dagger\hat{a}_\theta + e^{-i\varphi}\hat{a}_\theta^\dagger\hat{a}_\rho)^2 + \sin^2(\theta)\hat{n}_\rho\hat{n}_\theta \\
&\quad - \frac{1}{2}\cos(\theta)\sin(\theta)\left[(e^{i\varphi}\hat{a}_\rho^\dagger\hat{a}_\theta + e^{-i\varphi}\hat{a}_\theta^\dagger\hat{a}_\rho)(\hat{n}_\theta - \hat{n}_\rho) + h.c.\right] \\
&= (1 - \frac{1}{2}\sin^2(\theta))(\hat{n}_\theta^2 + \hat{n}_\rho^2) + \frac{1}{2}\sin^2(\theta)\left[e^{2i\varphi}(\hat{a}_\rho^\dagger)^2(\hat{a}_\theta)^2 + e^{-2i\varphi}(\hat{a}_\theta^\dagger)^2(\hat{a}_\rho)^2\right] + \frac{1}{2}\sin^2(\theta)(N + 4\hat{n}_\rho\hat{n}_\theta) \\
&\quad - \frac{1}{2}\cos(\theta)\sin(\theta)\left[(e^{i\varphi}\hat{a}_\rho^\dagger\hat{a}_\theta + e^{-i\varphi}\hat{a}_\theta^\dagger\hat{a}_\rho)(\hat{n}_\theta - \hat{n}_\rho) + h.c.\right] \equiv \hat{h}_2(\theta, \varphi). \tag{B4}
\end{aligned}$$

Using the Hamiltonian (B4) we can compute the exact universal functional close to the full BEC state along the radius  $\gamma_\rho$ , i.e., while keeping fixed the angles  $\theta$  and  $\varphi$ . In fact, close to that point, the wave function reads:

$$|\Psi_{\widetilde{\text{BEC}}}\rangle_\rho = \beta_0|N, 0\rangle_\rho \pm \beta_1|N - 2, 2\rangle_\rho, \tag{B5}$$

where  $\beta_0$  and  $\beta_1$  are taken real. Notice that the state (B5) gives place to a 1-RDM with  $\beta_1^2 = N/4 - \gamma_\rho/2$ . At the same time, the expectation value of the particles outside the condensate is  $\langle\Psi_{\widetilde{\text{BEC}}}\rangle_\rho \hat{n}_\theta |\Psi_{\widetilde{\text{BEC}}}\rangle_\rho = 2\beta_1^2$ . Let us take this as the important parameter  $\delta_\rho \equiv 2\beta_1^2 = N/2 - \gamma_\rho$ .

Our goal is to compute the expectation value  $\langle\Psi_{\widetilde{\text{BEC}}}\rangle_\rho \hat{h}_2(\theta, \varphi) |\Psi_{\widetilde{\text{BEC}}}\rangle_\rho$ . In order to do so we shall pre-compute the following expectation values:

$$\langle\Psi_{\widetilde{\text{BEC}}}\rangle_\rho (\hat{n}_\theta^2 + \hat{n}_\rho^2) |\Psi_{\widetilde{\text{BEC}}}\rangle_\rho = N^2 + 4\beta_1^2(2 - N) = N^2 - 2\delta_\rho(N - 2) \tag{B6}$$

and

$$\langle\Psi_{\widetilde{\text{BEC}}}\rangle_\rho \hat{n}_\rho \hat{n}_\theta |\Psi_{\widetilde{\text{BEC}}}\rangle_\rho = \beta_1^2 2(N - 2) = (N - 2)\delta_\rho. \tag{B7}$$

Since  $\langle N - 2, 2 |_\rho (\hat{a}_\rho^\dagger)^2 (\hat{a}_\theta)^2 | N, 0 \rangle_\rho = \sqrt{2N(N - 1)}$  we also have

$$\begin{aligned}
\langle\Psi_{\widetilde{\text{BEC}}}\rangle_\rho \left[ e^{2i\varphi}(\hat{a}_\rho^\dagger)^2 (\hat{a}_\theta)^2 + e^{-2i\varphi}(\hat{a}_\theta^\dagger)^2 (\hat{a}_\rho)^2 \right] |\Psi_{\widetilde{\text{BEC}}}\rangle_\rho &= \pm 2\cos(\varphi)\beta_0\beta_1\sqrt{2N(N - 1)} \\
&= \pm 2\cos(\varphi)\sqrt{\left(1 - \frac{\delta_\rho}{2}\right)}\delta_\rho\sqrt{N(N - 1)}. \tag{B8}
\end{aligned}$$

Collecting (B6), (B7) and (B8) we eventually arrive at:

$$\begin{aligned}
&\langle\Psi_{\widetilde{\text{BEC}}}\rangle_\rho (\hat{n}_l^2 + \hat{n}_r^2) |\Psi_{\widetilde{\text{BEC}}}\rangle_\rho \\
&= N^2 - 2(N - 2)\delta_\rho - \frac{1}{2}\sin^2(\theta)[N(N - 1) - 6(N - 2)\delta_\rho] \pm \sin^2(\theta)\cos(\varphi)\sqrt{N(N - 1)}\sqrt{\delta_\rho\left(1 - \frac{\delta_\rho}{2}\right)}. \tag{B9}
\end{aligned}$$

After executing the constrained search for ( $U > 0$ ), this result can be written in a much more insightful way

$$\mathcal{F}_N(\delta_\rho, \theta, \varphi) = \left[ E^0(\theta) - \sin^2(\theta)\cos(\varphi)\sqrt{N(N - 1)}\sqrt{\delta_\rho} + E^1(\theta)\delta_\rho + E^{3/2}(\theta, \varphi)\delta_\rho^{3/2} + \mathcal{O}(\delta_\rho^{5/2}) \right], \tag{B10}$$

where  $E^0(\theta) = N(N - 1) - \frac{1}{2}N(N - 1)\sin^2(\theta)$ ,  $E^1(\theta) = -2(N - 2) + 3(N - 2)\sin^2(\theta)$ , and

$$E^{3/2}(\theta, \varphi) = \frac{1}{4}\sqrt{N(N - 1)}\sin^2(\theta)\cos(\varphi).$$

Now we should compute the expectation value of the operator  $\hat{J}_z$ . To do so note that

$$\hat{J}_z = \frac{1}{2}(b_l^\dagger b_l - b_r^\dagger b_r) = \cos(\theta) \frac{1}{2}(a_\rho^\dagger a_\rho - a_\theta^\dagger a_\theta). \quad (\text{B11})$$

Therefore,

$$\langle \widetilde{\Psi}_{\text{BEC}} | \hat{J}_z | \widetilde{\Psi}_{\text{BEC}} \rangle_\rho = \left( \frac{N}{2} - \delta_\rho \right) \cos(\theta), \quad (\text{B12})$$

as expected from the definition of  $\gamma_z$ . Collecting the Eq. (B10) and (B12) we finally have

$$\mathcal{M}_{zz}[\gamma] = 2\mathcal{F}[\gamma] - 4\gamma_z^2 - N^2 + 2N = N \sin^2(\theta) - 2 \sin^2(\theta) \cos(\varphi) \sqrt{N(N-1)} \sqrt{\delta_\rho} + \tilde{E}^1(\theta) \delta_\rho + \mathcal{O}(\delta_\rho^{3/2}), \quad (\text{B13})$$

where  $\tilde{E}^1(\theta) = 8 + 2(N-6) \sin^2(\theta)$ .

The rest of the matricial elements of the QFIM can be computed along similar lines.

### Appendix C: Derivative of the functional

To prove Eq. (9) we first need to show that for ground states:

$$\frac{\partial \mathcal{F}[\mathbf{u}; \gamma]}{\partial u_{\alpha\beta}} = \langle \psi[\gamma] | \frac{\hat{W}(\mathbf{u})}{\partial u_{\alpha\beta}} | \psi[\gamma] \rangle, \quad (\text{C1})$$

where we assume that the derivative keeps fixed  $\gamma$ . To that aim, let's first use the fact that the Hamiltonian can be written as  $\hat{H}(\mathbf{u}) = \hat{h} + \hat{W}(\mathbf{u})$ , where  $\hat{h}$  is the one-particle Hamiltonian. Thus, we have:

$$\mathcal{F}[\mathbf{u}; \gamma] = \langle \psi[\gamma] | \hat{W}(\mathbf{u}) | \psi[\gamma] \rangle = \langle \psi[\gamma] | \hat{H}(\mathbf{u}) | \psi[\gamma] \rangle - \langle \psi[\gamma] | \hat{h} | \psi[\gamma] \rangle. \quad (\text{C2})$$

It follows that

$$\frac{\partial \mathcal{F}[\mathbf{u}; \gamma]}{\partial u_{\alpha\beta}} = \frac{\partial}{\partial u_{\alpha\beta}} \langle \psi[\gamma] | \hat{H}(\mathbf{u}) | \psi[\gamma] \rangle - \frac{\partial}{\partial u_{\alpha\beta}} \langle \psi[\gamma] | \hat{h} | \psi[\gamma] \rangle. \quad (\text{C3})$$

Due to the Hellmann–Feynman theorem the first term gives (recall that the wave functions are ground states)

$$\frac{\partial}{\partial u_{\alpha\beta}} \langle \psi[\gamma] | \hat{H}(\mathbf{u}) | \psi[\gamma] \rangle = \langle \psi[\gamma] | \frac{\partial \hat{H}(\mathbf{u})}{\partial u_{\alpha\beta}} | \psi[\gamma] \rangle. \quad (\text{C4})$$

The second term gives

$$\frac{\partial}{\partial u_{\alpha\beta}} \langle \psi[\gamma] | \hat{h} | \psi[\gamma] \rangle = \frac{\partial}{\partial u_{\alpha\beta}} \text{Tr}[\hat{h}\gamma]. \quad (\text{C5})$$

But since we have assumed that  $\gamma$  is kept fixed while performing the derivative, this term is zero. As a result,

$$\frac{\partial \mathcal{F}[\mathbf{u}; \gamma]}{\partial u_{\alpha\beta}} = \langle \psi[\gamma] | \frac{\partial \hat{H}(\mathbf{u})}{\partial u_{\alpha\beta}} | \psi[\gamma] \rangle = \langle \psi[\gamma] | \frac{\partial \hat{W}(\mathbf{u})}{\partial u_{\alpha\beta}} | \psi[\gamma] \rangle. \quad (\text{C6})$$

which is what we wanted to prove.

[1] R. Islam, R. Ma, P. M. Preiss, M. Eric Tai, A. Lukin, M. Rispoli, and M. Greiner, Measuring entanglement entropy in a quantum many-body system, *Nature* **528**, 77 (2015).

[2] A. Bergschneider, V. Klinkhamer, J. Becher, R. Klemt, L. Palm, G. Zürn, S. Jochim, and P. Preiss, Experimental characterization of two-particle entanglement through position and momentum correlations, *Nat. Phys.* **15**, 640 (2019).

- [3] Z. Huang and S. Kais, Entanglement as measure of electron–electron correlation in quantum chemistry calculations, *Chem. Phys. Lett.* **413**, 1 (2005).
- [4] C. L. Benavides-Riveros, N. N. Lathiotakis, and M. A. L. Marques, Towards a formal definition of static and dynamic electronic correlations, *Phys. Chem. Chem. Phys.* **19**, 12655 (2017).
- [5] P. Calabrese and J. Cardy, Entanglement entropy and conformal field theory, *J. Phys. A: Math. Theor.* **42**, 504005 (2009).
- [6] T. Nishioka, S. Ryu, and T. Takayanagi, Holographic entanglement entropy: an overview, *J. Phys. A: Math. Theor.* **42**, 504008 (2009).
- [7] M. Paris, Quantum estimation for quantum technology, *Int. J. Quantum Inf.* **07**, 125 (2009).
- [8] A. Rath, C. Branciard, A. Minguzzi, and B. Vermersch, Quantum Fisher Information from Randomized Measurements, *Phys. Rev. Lett.* **127**, 260501 (2021).
- [9] L. Pezzè and A. Smerzi, Entanglement, nonlinear dynamics, and the heisenberg limit, *Phys. Rev. Lett.* **102**, 100401 (2009).
- [10] G. Tóth, Multipartite entanglement and high-precision metrology, *Phys. Rev. A* **85**, 022322 (2012).
- [11] R. Costa de Almeida and P. Hauke, From entanglement certification with quench dynamics to multipartite entanglement of interacting fermions, *Phys. Rev. Res.* **3**, L032051 (2021).
- [12] U. Marzolino and T. Prosen, Fisher information approach to nonequilibrium phase transitions in a quantum XXZ spin chain with boundary noise, *Phys. Rev. B* **96**, 104402 (2017).
- [13] P. Hauke, M. Heyl, L. Tagliacozzo, and P. Zoller, Measuring multipartite entanglement through dynamic susceptibilities, *Nat. Phys.* **12**, 778 (2016).
- [14] A. J. Daley, H. Pichler, J. Schachenmayer, and P. Zoller, Measuring Entanglement Growth in Quench Dynamics of Bosons in an Optical Lattice, *Phys. Rev. Lett.* **109**, 020505 (2012).
- [15] A. Niezgoda and J. Chwedeńczuk, Many-Body Nonlocality as a Resource for Quantum-Enhanced Metrology, *Phys. Rev. Lett.* **126**, 210506 (2021).
- [16] M. Gärttner, P. Hauke, and A. M. Rey, Relating Out-of-Time-Order Correlations to Entanglement via Multiple-Quantum Coherences, *Phys. Rev. Lett.* **120**, 040402 (2018).
- [17] J. Lambert and E. S. Sørensen, From classical to quantum information geometry: a guide for physicists, *New J. Phys.* **25**, 081201 (2023).
- [18] G. Tóth and I. Apellaniz, Quantum metrology from a quantum information science perspective, *J. Phys. A: Math. Theor.* **47**, 424006 (2014).
- [19] J. Liu, H. Yuan, X.-M. Lu, and X. Wang, Quantum Fisher information matrix and multiparameter estimation, *J. Phys. A: Math. Theor.* **53**, 023001 (2019).
- [20] L. J. Fiderer, J. M. E. Fraïsse, and D. Braun, Maximal Quantum Fisher Information for Mixed States, *Phys. Rev. Lett.* **123**, 250502 (2019).
- [21] E. Romera and J. S. Dehesa, The Fisher–Shannon information plane, an electron correlation tool, *J. Chem. Phys.* **120**, 8906 (2004).
- [22] L. Pezzè, A. Smerzi, M. K. Oberthaler, R. Schmied, and P. Treutlein, Quantum metrology with nonclassical states of atomic ensembles, *Rev. Mod. Phys.* **90**, 035005 (2018).
- [23] J. L. Beckey, M. Cerezo, A. Sone, and P. J. Coles, Variational quantum algorithm for estimating the quantum Fisher information, *Phys. Rev. Res.* **4**, 013083 (2022).
- [24] H. Strobel, W. Muessel, D. Linnemann, T. Zibold, D. B. Hume, L. Pezzè, A. Smerzi, and M. Oberthaler, Fisher information and entanglement of non-Gaussian spin states, *Science* **345**, 424 (2014).
- [25] B. Lücke, M. Scherer, J. Kruse, L. Pezzè, F. Deuretzbacher, P. Hyllus, O. Topic, J. Peise, W. Ertmer, J. Arlt, L. Santos, A. Smerzi, and C. Klempt, Twin Matter Waves for Interferometry Beyond the Classical Limit, *Science* **334**, 773 (2011).
- [26] G. Mathew, S. Silva, A. Jain, A. Mohan, D. T. Adroja, V. G. Sakai, C. V. Tomy, A. Banerjee, R. Goreti, A. V. N., R. Singh, and D. Jaiswal-Nagar, Experimental realization of multipartite entanglement via quantum Fisher information in a uniform antiferromagnetic quantum spin chain, *Phys. Rev. Res.* **2**, 043329 (2020).
- [27] M. Yu, Y. Liu, P. Yang, M. Gong, Q. Cao, S. Zhang, H. Liu, M. Heyl, T. Ozawa, N. Goldman, *et al.*, Quantum Fisher information measurement and verification of the quantum Cramér–Rao bound in a solid-state qubit, *npj Quantum Inf.* **8**, 56 (2022).
- [28] J. T. Reilly, J. D. Wilson, S. B. Jäger, C. Wilson, and M. J. Holland, Optimal generators for quantum sensing, *Phys. Rev. Lett.* **131**, 150802 (2023).
- [29] D.-L. Deng, Machine Learning Detection of Bell Nonlocality in Quantum Many-Body Systems, *Phys. Rev. Lett.* **120**, 240402 (2018).
- [30] J. Batle, C. H. R. Ooi, S. Abdalla, and A. Bagdasaryan, Computing the maximum violation of a Bell inequality is an NP-problem, *Quantum Inf. Process.* **15**, 2649 (2016).
- [31] F. Aikebaier, T. Ojanen, and J. Lado, Extracting electronic many-body correlations from local measurements with artificial neural networks, *SciPost Phys. Core* **6**, 030 (2023).
- [32] J. R. Moreno, G. Carleo, and A. Georges, Deep Learning the Hohenberg-Kohn Maps of Density Functional Theory, *Phys. Rev. Lett.* **125**, 076402 (2020).
- [33] X. Shao, L. Paetow, M. E. Tuckerman, and M. Pavanello, Machine learning electronic structure methods based on the one-electron reduced density matrix, *Nat. Commun.* **14**, 6281 (2023).
- [34] A. Grisafi, A. Lewis, M. Rossi, and M. Ceriotti, Electronic-Structure Properties from Atom-Centered Predictions of the Electron Density, *J. Chem. Theory Comput.* **19**, 4451 (2023).
- [35] F. Aikebaier, T. Ojanen, and J. L. Lado, Machine learning the Kondo entanglement cloud from local measurements (2023), [arXiv:2311.07253](https://arxiv.org/abs/2311.07253).
- [36] P. Hohenberg and W. Kohn, Inhomogeneous electron gas, *Phys. Rev.* **136**, B864 (1964).
- [37] U. von Barth and L. Hedin, A local exchange-correlation potential for the spin polarized case. i, *J. Phys. C: Solid State Phys.* **5**, 1629 (1972).
- [38] W. Kohn, A. Savin, and C. Ullrich, Hohenberg–Kohn theory including spin magnetism and magnetic fields, *Int. J. Quantum Chem.* **101**, 20 (2005).
- [39] T. L. Gilbert, Hohenberg-Kohn theorem for nonlocal external potentials, *Phys. Rev. B* **12**, 2111 (1975).
- [40] J. Schmidt, C. L. Benavides-Riveros, and M. A. L. Marques, Reduced density matrix functional theory for superconductors, *Phys. Rev. B* **99**, 224502 (2019).

- [41] S. Goedecker and C. J. Umrigar, Natural Orbital Functional for the Many-Electron Problem, *Phys. Rev. Lett.* **81**, 866 (1998).
- [42] R. O. Jones, Density functional theory: Its origins, rise to prominence, and future, *Rev. Mod. Phys.* **87**, 897 (2015).
- [43] M. Piris, Global Natural Orbital Functional: Towards the Complete Description of the Electron Correlation, *Phys. Rev. Lett.* **127**, 233001 (2021).
- [44] M. Piris, Global Method for Electron Correlation, *Phys. Rev. Lett.* **119**, 063002 (2017).
- [45] J. Cioslowski, *Many-Electron Densities and Reduced Density Matrices* (Springer New York, NY, 2000).
- [46] K. Pernal, Effective Potential for Natural Spin Orbitals, *Phys. Rev. Lett.* **94**, 233002 (2005).
- [47] E. J. Baerends, Exact exchange-correlation treatment of dissociated  $h_2$  in density functional theory, *Phys. Rev. Lett.* **87**, 133004 (2001).
- [48] J. Cioslowski, C. Schilling, and R. Schilling, 1-Matrix functional for long-range interaction energy of two hydrogen atoms, *J. Chem. Phys.* **158**, 084106 (2023).
- [49] P. Mori-Sánchez and A. J. Cohen, Exact Density Functional Obtained via the Levy Constrained Search, *J. Phys. Chem. Lett.* **9**, 4910 (2018).
- [50] S. Sharma, J. K. Dewhurst, S. Shallcross, and E. K. U. Gross, Spectral density and metal-insulator phase transition in mott insulators within reduced density matrix functional theory, *Phys. Rev. Lett.* **110**, 116403 (2013).
- [51] J. A. Martinez B, X. Shao, K. Jiang, and M. Pavanello, Entropy is a good approximation to the electronic (static) correlation energy, *J. Chem. Phys.* **159**, 191102 (2023).
- [52] J. Wang and E. J. Baerends, Self-Consistent-Field Method for Correlated Many-Electron Systems with an Entropic Cumulant Energy, *Phys. Rev. Lett.* **128**, 013001 (2022).
- [53] O. Dutta, M. Gajda, P. Hauke, M. Lewenstein, D.-S. Lühmann, B. A. Malomed, T. Sowiński, and J. Zakrzewski, Non-standard Hubbard models in optical lattices: a review, *Rep. Prog. Phys.* **78**, 066001 (2015).
- [54] K. Pernal and K. Giesbertz, Reduced Density Matrix Functional Theory (RDMFT) and Linear Response Time-Dependent RDMFT (TD-RDMFT), in *Density-Functional Methods for Excited States*, edited by N. Ferré, M. Filatov, and M. Huix-Rotllant (Springer International Publishing, Cham, 2016) p. 125.
- [55] Eventually, the functional depends also on the chosen (fermionic/bosonic) statistics of the problem and the total number of particles. Consequently, for a specific problem fixed by  $\hbar$ , the relevant 1-RDM fulfills the equation  $\nabla_{\gamma} \mathcal{F}[\gamma] = -\hbar$  resulting from the minimization of  $\mathcal{E}[\gamma]$ .
- [56] M. Levy, Universal variational functionals of electron densities, first-order density matrices, and natural spin-orbitals and solution of the  $v$ -representability problem, *Proc. Natl. Acad. Sci. U.S.A.* **76**, 6062 (1979).
- [57] C. L. Benavides-Riveros, J. Wolff, M. A. L. Marques, and C. Schilling, Reduced Density Matrix Functional Theory for Bosons, *Phys. Rev. Lett.* **124**, 180603 (2020).
- [58] J. Liebert and C. Schilling, Functional theory for Bose-Einstein condensates, *Phys. Rev. Res.* **3**, 013282 (2021).
- [59] T. Maciazek, Repulsively diverging gradient of the density functional in the reduced density matrix functional theory, *New J. Phys.* **23**, 113006 (2021).
- [60] J. Schmidt, M. Fadel, and C. L. Benavides-Riveros, Machine learning universal bosonic functionals, *Phys. Rev. Res.* **3**, L032063 (2021).
- [61] C. Schilling and R. Schilling, Diverging Exchange Force and Form of the Exact Density Matrix Functional, *Phys. Rev. Lett.* **122**, 013001 (2019).
- [62] A. J. Cohen and P. Mori-Sánchez, Landscape of an exact energy functional, *Phys. Rev. A* **93**, 042511 (2016).
- [63] In the literature of functional theory the minimizers of the constrained-search are called  $v$ -representable when they correspond to the ground state of some Hamiltonian (with the same  $W$ ) or non- $v$ -representable when they not. The concept of  $N$ -representability refers to 1-RDMs that come from at least one  $N$ -particle quantum state.
- [64] S. L. Braunstein and C. M. Caves, Statistical distance and the geometry of quantum states, *Phys. Rev. Lett.* **72**, 3439 (1994).
- [65] A. Holevo, *Probabilistic and Statistical Aspects of Quantum Theory*, Publications of the Scuola Normale Superiore (Scuola Normale Superiore, 2011).
- [66] C. L. Degen, F. Reinhard, and P. Cappellaro, Quantum sensing, *Rev. Mod. Phys.* **89**, 035002 (2017).
- [67] P. Hyllus, W. Laskowski, R. Krischek, C. Schwemmer, W. Wieczorek, H. Weinfurter, L. Pezzé, and A. Smerzi, Fisher information and multiparticle entanglement, *Phys. Rev. A* **85**, 022321 (2012).
- [68] P. Gersdorf, W. John, J. P. Perdew, and P. Ziesche, Correlation entropy of the H2 molecule, *Int. J. Quantum Chem.* **61**, 935 (1997).
- [69] M. Tichy, F. Mintert, and A. Buchleitner, Essential entanglement for atomic and molecular physics, *J. Phys. B: At. Mol. Opt. Phys.* **44**, 192001 (2011).
- [70] C. L. Benavides-Riveros, I. V. Toranzo, and J. S. Dehesa, Entanglement in  $N$ -harmonium: bosons and fermions, *J. Phys. B: At. Mol. Opt. Phys.* **47**, 195503 (2014).
- [71] S. M. Sutter and K. J. H. Giesbertz, One-body reduced density-matrix functional theory for the canonical ensemble, *Phys. Rev. A* **107**, 022210 (2023).
- [72] K. Giesbertz and M. Ruggenthaler, One-body reduced density-matrix functional theory in finite basis sets at elevated temperatures, *Phys. Rep.* **806**, 1 (2019).
- [73] M. Rodríguez-Mayorga, K. J. Giesbertz, and L. Visscher, Relativistic reduced density matrix functional theory., *SciPost Chem.* **1**, 004 (2022).
- [74] C. L. Benavides-Riveros and M. A. L. Marques, On the time evolution of fermionic occupation numbers, *J. Chem. Phys.* **151**, 044112 (2019).
- [75] S. Di Sabatino, C. Verdozzi, and P. Romaniello, Time dependent reduced density matrix functional theory at strong correlation: insights from a two-site Anderson impurity model, *Phys. Chem. Chem. Phys.* **23**, 16730 (2021).
- [76] J. Liebert and C. Schilling, Deriving density-matrix functionals for excited states, *SciPost Phys.* **14**, 120 (2023).
- [77] A. Görling, Density-functional theory beyond the Hohenberg-Kohn theorem, *Phys. Rev. A* **59**, 3359 (1999).
- [78] D. J. Carrascal, J. Ferrer, J. C. Smith, and K. Burke, The Hubbard dimer: a density functional case study of a many-body problem, *J. Phys.: Cond. Matt.* **27**, 393001 (2015).
- [79] D. J. Carrascal, J. Ferrer, N. Maitra, and K. Burke, Linear response time-dependent density functional theory of the Hubbard dimer, *Eur. Phys. J. B* **91**, 142 (2018).
- [80] K. Deur and E. Fromager, Ground and excited energy levels can be extracted exactly from a single ensemble density-functional theory calculation, *J. Chem. Phys.* **150**, 094106 (2019).

- [81] J. Liebert, A. Y. Chaou, and C. Schilling, Refining and relating fundamentals of functional theory, *J. Chem. Phys.* **158**, 214108 (2023).
- [82] C. L. Benavides-Riveros, Orbital-free quasi-density functional theory, [arXiv:2304.09056](https://arxiv.org/abs/2304.09056) (2023).
- [83] R. Alicki, M. Horodecki, A. Jenkins, M. Łobejko, and G. Suárez, The Josephson junction as a quantum engine, *New J. Phys.* **25**, 113013 (2023).
- [84] R. Schmied, J.-D. Bancal, B. Allard, M. Fadel, V. Scarani, P. Treutlein, and N. Sangouard, Bell correlations in a Bose-Einstein condensate, *Science* **352**, 441 (2016).
- [85] M. Fadel, T. Zibold, B. Décamps, and P. Treutlein, Spatial entanglement patterns and Einstein-Podolsky-Rosen steering in Bose-Einstein condensates, *Science* **360**, 409 (2018).
- [86] J. Ma, X. Wang, C. Sun, and F. Nori, Quantum spin squeezing, *Phys. Rep.* **509**, 89 (2011).
- [87] D. Dast, D. Haag, H. Cartarius, and G. Wunner, Purity oscillations in Bose-Einstein condensates with balanced gain and loss, *Phys. Rev. A* **93**, 033617 (2016).
- [88] O. Penrose and L. Onsager, Bose-Einstein Condensation and Liquid Helium, *Phys. Rev.* **104**, 576 (1956).